

## Contributions of Crystallography to Materials Science\*

*Hartmut Fuess*

*Fachgebiet Strukturforchung, Fachbereich Materialwissenschaft, Technische Hochschule Darmstadt, Petersenstraße 23, 64287 Darmstadt, Germany*

Received March 26, 1996; revised June 24, 1996; accepted July 10, 1996

The properties of materials used in various domains of science and engineering are directly correlated to the microstructure. Crystallography is devoted to the investigation of microstructure of substances and materials by a variety of diffraction and spectroscopic methods. Several examples related to research in the department of materials science at the Technical University of Darmstadt are presented. The structure and dynamics of aromatic host molecules in catalytically active zeolites are investigated by X-ray and neutron diffraction and NMR-spectroscopy combined with inelastic neutron scattering. Surfaces and interfaces of semiconductors and thin superconducting films are studied by grazing incidence techniques. By examination of the reflectogram details on thickness, composition, surface roughness and a possible modification of these values are obtained.

Transmission electron microscopy provides complementary information on the structure of interfaces, especially through the support of simulated images by a multi-slice method. Work is presented on CoSi<sub>2</sub>-films on Si and wafers of GaAs with LaB<sub>6</sub> films. Modification of these wafers by ion mixing techniques is attempted. Furthermore, surface hardening of steel by ion implantation (carbon and nitrogen) is a way of improving tribological properties. Grazing incidence provides results on the formation of different carbides as a function of depth. Superconducting films of Bi<sub>2</sub>Sr<sub>2</sub>CaCu<sub>2</sub>O<sub>8</sub> on SrTiO<sub>3</sub> showed an improvement by a factor of 10 in critical current density by creating holes (Xe, Au, U-irradiation) as pinning centres. The examination by TEM revealed an amorphization of the channels with clear boundaries between the channel and nonirradiated material.

---

\* Based upon the lecture presented at the Fourth Croatian-Slovenian Crystallographic Meeting, Trakošćan, Croatia, Sept 28 – Sept 30, 1995.

## INTRODUCTION

The development of »new materials« constitutes an important challenge in various fields of science and engineering. Whereas the preparative chemist invents new substances, the engineer on the other end of the scale wants a well characterized material with known structure and properties.

Crystallography has invented a wide range of techniques which are instrumental in the procedure from a chemical substance into a material. Many of these techniques are based on X-ray diffraction but electron microscopy, neutron scattering or spectroscopic methods have made important contributions. It is not the intention of the present paper to give a comprehensive review of all these fields. We shall present some examples that are related to the present research work of our laboratory. Additional information on the application of X-ray crystallography in chemistry is given in a volume devoted to the celebration of the detection of X-rays in 1895 by Röntgen.<sup>1</sup>

We shall report here mainly on X-ray techniques devoted to the characterization of surfaces and interfaces and describe the complementary use of electron microscopy in this field. We shall add a chapter on the magnetic properties of superconducting material and a brief summary of our results on host-guest interactions in micro- und mesoporous zeolites.

## HOST-GUEST INTERACTION IN ZEOLITES

Whereas the channels and voids of natural zeolites are filled with cations and water molecules, catalytically active materials are produced by either ion exchange of natural species or by direct synthesis.

A great variety of ions or organic molecules may be introduced into the cavities and thus materials for different applications are produced. The decomposition of  $\text{Pt}(\text{NH}_3)_4^{2+}$  in zeolite NaX yields nanocrystalline platinum clusters applicable in catalysis.<sup>2</sup>

Adsorption of dye molecules produces pigments.<sup>3</sup>

Polar aromatic molecules like nitroaniline are of potential use for non-linear optics (NLO). As demonstrated by Caro *et al.*,<sup>4</sup> the alignment of these molecules in the channels of zeolites is feasible and produces a NLO-effect. A more detailed review of zeolitic materials has been given by Kaučič in this journal.<sup>5</sup>

The framework of zeolites consists of  $\text{TO}_4$ -tetrahedra, where  $\text{T} = \text{Si}, \text{Al}$  in natural species. The tetrahedra are connected by common oxygen atoms. The charge balance is achieved by cations like Na, Ca, Ba, K in the voids. The technical application requires introduction of organic molecules into the holes.

Our investigations are concerned with the structure and dynamics of these aromatic molecules in faujasite type zeolites. Figure 1 shows diffraction patterns of *m*-dinitrobenzene in zeolite NaY by X-ray (Figure 1a) and neutron diffraction (Figure 1b). The difference curve presented in the figures below the observed pattern is due to the contribution of the aromatic molecule. The molecule was located by a grid-method, which allowed a careful search of reciprocal space in the relevant density map. The full pattern was refined by Rietveld difference techniques. The position of the molecule is presented in Figure 2.<sup>6</sup> Furthermore, the position of the molecules within the zeolite was calculated based on molecular mechanic models and reasonable agreement was obtained for xylenes, toluenes<sup>7</sup> and nitrobenzenes.<sup>6</sup>

Whereas diffraction techniques present only the static position of a molecule in the channel of zeolites, the dynamics and the motion are studied by spectroscopic methods. Nuclear magnetic resonance<sup>8</sup> and inelastic neutron scattering<sup>9</sup> cover different time-scales and are, therefore, complementary for a detailed investigation of the dynamics.

Thus, a complete picture of the motion of paraxylene in zeolite NaX has been established. Whereas the whole molecule moves almost freely at room temperature in the channel, freezing in of the aromatic molecule is observed at about 160 K but the two CH<sub>3</sub>-groups still rotate and their motion persists down to 4 K, as found by quasielastic neutron scattering.

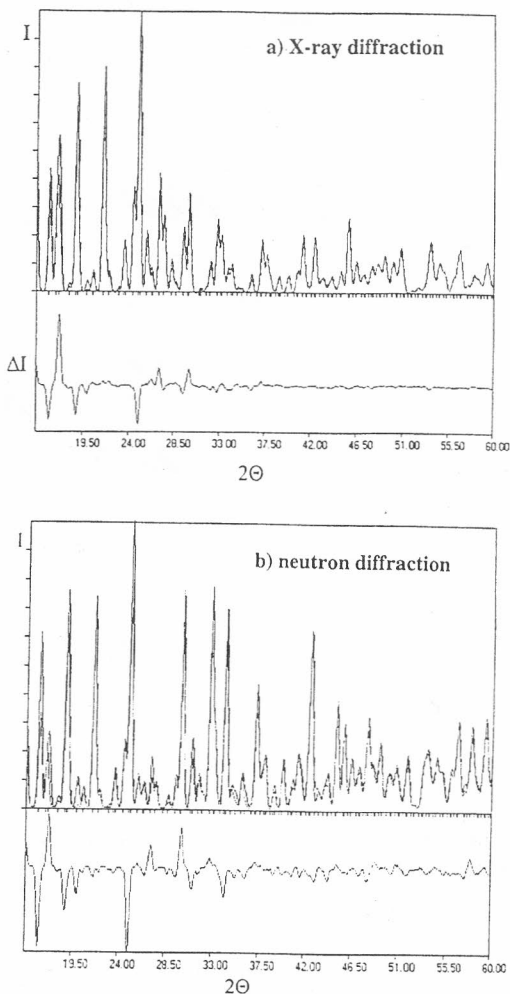


Figure 1. a) X-ray diffraction pattern of zeolite NaY loaded with *m*-dinitro benzene, b) neutron diffraction of the same material. The intensity difference due to aromatic molecules is shown below.

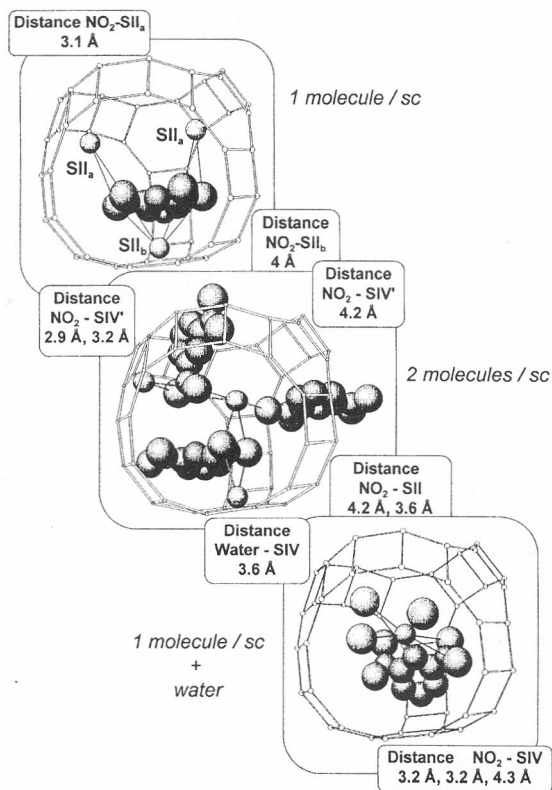


Figure 2. Arrangement of *m*-dinitrobenzene in the supercage of faujasite NaY, different loadings and water content.

## SURFACE X-RAY DIFFRACTION

The characterization of surfaces and interfaces is a prerequisite for the preparation of a variety of materials, especially for semiconductors but also for the whole class of nanostructured materials. Whereas X-ray techniques are non-destructive, the preparation techniques for transmission electron microscopy (TEM) studies need preparation techniques that may modify the specimen.

### *Reflectometry*

Investigation of the surfaces of materials by X-ray diffraction is determined by absorption and reflectivity of this radiation. The method is based

on the index of refraction of the material under study and of the differences in this index between materials.

$$n = 1 - \delta + i\beta$$

where  $\delta$  is proportional to the the real part ( $f'$ ) and  $\beta$  proportional to the imaginary part ( $f''$ ) of the atomic form factor ( $f = f_o + f' + if''$ ). The numerical value of the refractive index is slightly smaller than unity, *e.g.* for Fe and  $\text{CuK}\alpha$  - radiation  $n = 0.9975$ . Any material is therefore less dense than air for the scattering of X-rays from surfaces hence total reflection occurs for small angles of incidence. The critical angle for total reflection is given as

$$\theta_c = \sqrt{2\delta}$$

and amounts to several minutes (*e.g.*  $\theta_c = 37'$  for Fe) for most surfaces. Above the critical angle, radiation penetrates into the material and is reflected at any new interface. X-rays reflected at the surface and at interfaces may interfere and produce a reflectogram, as presented in Figure 3. Evidently, the interference depends on the thickness of the film, which is thus easily determined from the pattern. Furthermore, information on the density of the material and on the roughness of surfaces and interfaces may be deduced. Reflectometry requires fairly smooth and regular surfaces and is therefore widely applied for the investigation of semiconductors. Figure 4

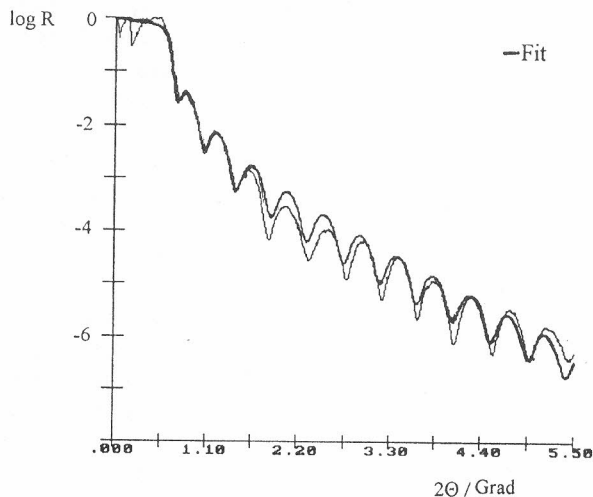


Figure 3. Reflectivity ( $\log R$ ) as a function of the angle of incidence for  $\text{CoSi}_2$  on Si. Comparison of experimental and fitted curves. Thickness of  $\text{CoSi}_2$  (19.6 nm), roughness (3.2 Å surface, 3.4 Å interface).

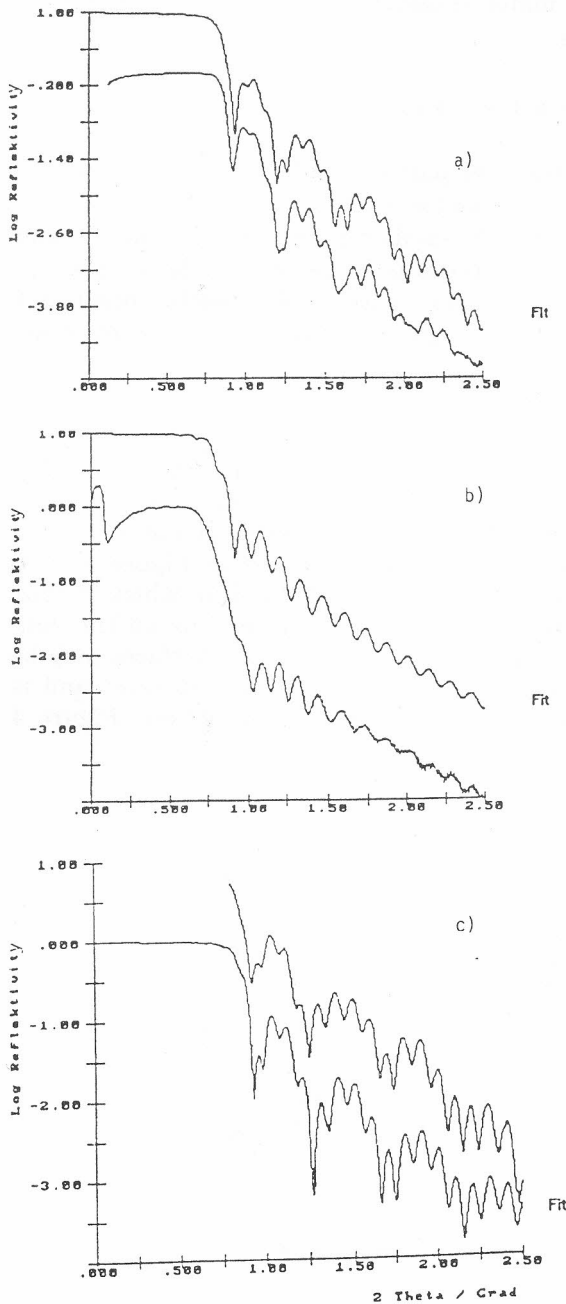


Figure 4. Reflectometry of LaB<sub>6</sub> on GaAs; a) as prepared; b) 700 °C, 5 s; c) 500 °C, 30 s.

gives two reflectograms from a wafer prepared by molecular beam epitaxy of LaB<sub>6</sub> on GaAs with an additional covering preparation of Ni. Figure 4a presents the untreated, as prepared sample and Figure 4b after thermal treatment at 700 °C for 5 sec. The thickness in both cases of the various layers is fairly similar, as indicated in the figure, the difference in the curve stems from a considerable roughness in the non-treated, as prepared material (Figure 4a). The angle of total reflection is clearly indicated in both figures. The experimental patterns are fitted and thickness, roughness, and density are applied as fit parameters. In the case of Figure 4b, the fit revealed a new additional layer between LaB<sub>6</sub> and GaAs. Diffraction experiments at grazing incidence produced Bragg peaks which were indexed as LaAs. Tempering at 700 °C did change the pattern but not the presence of that layer whereas a thermal treatment for 30 sec at 500 °C (Figure 4c) resulted in a product that did not show any intermediate layer. So, direct evidence, non-destructive, of the presence of a new phase and of the optimal conditions for the preparation of the wafer was obtained.<sup>10</sup>

*Grazing incidence diffraction*

Due to absorption, the penetration of X-rays in material is limited but still amounts to several  $\mu\text{m}$  for Cu  $K\alpha$  radiation. It is therefore not normally suited for an investigation of surface effects. But at low incidence angles, the dependence of the penetration length  $p$  may be varied as a function of the incidence angle  $\alpha$

$$p \approx \sin \alpha / \mu \delta$$

with  $\mu$  the linear absorption coefficient and  $\delta$  the density of the material. As the incidence angles are rather small, the method is known as grazing incidence. In Figure 5, a diffraction pattern obtained by grazing incidence on steel is displayed.<sup>11</sup>

Carbon atoms were implanted into the surface by an ion accelerator (50KeV and a dose of  $10^{18}$  atoms/cm<sup>2</sup>). It is evident from Figure 5a that carbides were produced in the surface and the adjacent layers as predominant species whereas martensitic steel is only detected at a depth of about 100 nm. The formation of carbides on the surface of a highly alloyed steel is known to improve the abrasive properties of steel. The grazing incidence method thus presents a valuable tool for studying the structural details of that improvement.

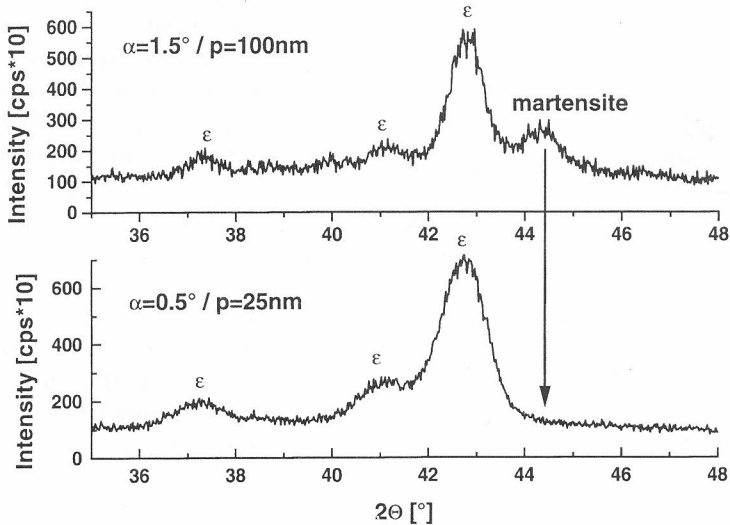


Figure 5. Grazing incidence measurement on highly alloyed steel. Above: penetration of 100 nm with  $\epsilon\text{-Fe}_3\text{C}$  and martensite, below: penetration of 25 nm showing only  $\epsilon\text{-Fe}_3\text{C}$ .

### Real structure of thin films

Thin films of ceramic high temperature superconductors are prepared by various methods (CVD = chemical vapour deposition,<sup>12</sup> laser ablation<sup>13</sup>) on different substrates. In the superconducting phase, films of  $\text{YBa}_2\text{Cu}_3\text{O}_{7-\delta}$  are crystalline with orthorhombic symmetry. Two reflections are due to the difference in the lattice constants ( $a = 3.82 \text{ \AA}$ ,  $b = 3.86 \text{ \AA}$ ) in the orthorhombic phase. The  $c$ -axis is perpendicular to the surface of substrate and film. The lattice constants of  $\text{SrTiO}_3$  ( $a = 3.905 \text{ \AA}$ ) and  $\text{NdGaO}_3$  produce a fairly good epitaxial growth. X-ray diffraction revealed (Figure 6) an additional splitting of each individual reflection, thus reflecting the twinning of the crystalline film. The precise form of the reflection is related to the interplay of the lattices in reciprocal space for the  $hk2$  lattice plane. The lattices correspond to two twin individuals, the twinning axis is  $[110]$ . These reflections were observed by  $\Psi$ -scans on a four-circle diffractometer<sup>14</sup> and  $\text{NdGaO}_3$  as substrate. A treatment of the superconducting film in reducing atmosphere produces a single spot which corresponds to the nonsuperconducting tetragonal phase. Subsequent treatment in oxygen brings the original picture hence the orthorhombic structure back (Figure 7, first row). The dependence of the real structure on the substrate is demonstrated in Figure 7 (second row) where  $\text{MgO}$  (lattice parameter  $a = 4.21 \text{ \AA}$ ) is used as a substrate. The relatively large differences in lattice constants between the deposited superconductor material and the substrate produce a smeared out electron density.

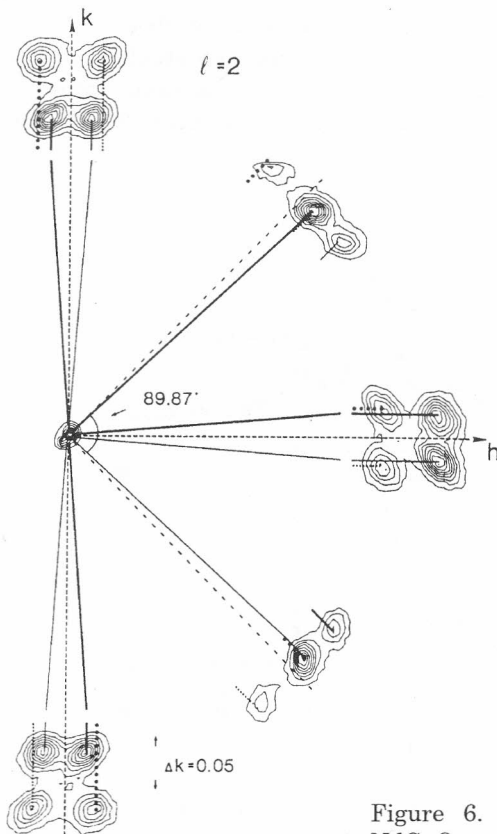


Figure 6. X-ray reflections of  $\text{YBa}_2\text{Cu}_3\text{O}_7$  and  $\text{NdGaO}_3$ - substrates. Splitting of reflections in the  $hk2$  plane.



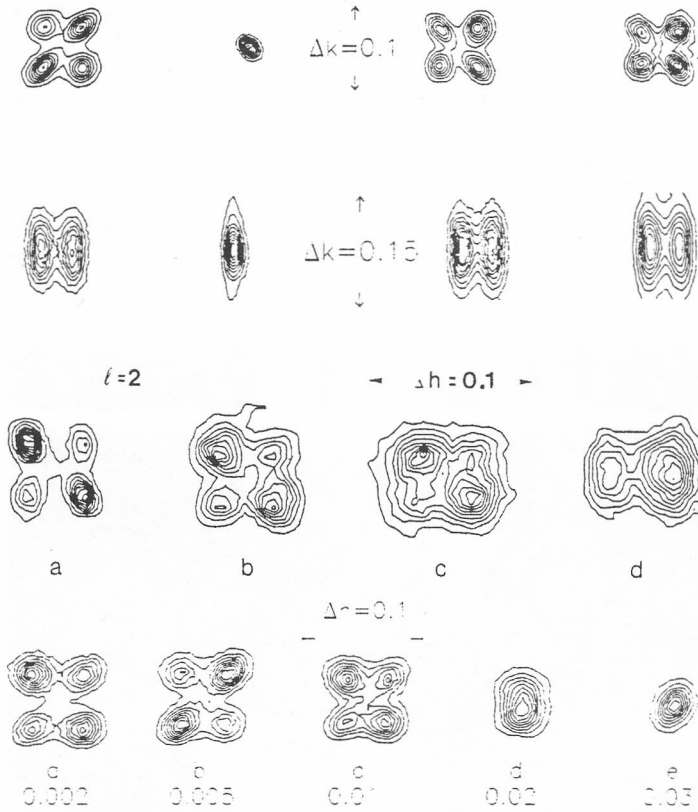


Figure 7. Splitting of YBCO-reflection on SrTiO<sub>3</sub>. First row: a) original; b) reduction in N<sub>2</sub>; c) reoxidation 12 h; d) reoxidation 24 h. Second row: YBCO on MgO, the same sequence as in the first row. Third row: Irradiation by <sup>209</sup>Bi 1.4 GeV, a) 302 – Reflection group; b) 10<sup>10</sup>/cm<sup>2</sup>; c) 10<sup>11</sup>/cm<sup>2</sup>; d) 5 × 10<sup>11</sup>/cm<sup>2</sup>. Fourth row: YBa<sub>2</sub>Cu<sub>3-x</sub>Fe<sub>x</sub>O<sub>7</sub>, a) x = 0.002; b) x = 0.005; c) x = 0.01; d) x = 0.02; e) x = 0.03.

Substitution of Cu by other 3d-elements or aluminium is known to destroy superconductivity. An amount of 3% Fe leads to a tetragonal symmetry (Figure 7 fourth row). This corresponds well with the orthorhombic-tetragonal transition observed for the powder of YBa<sub>2</sub>Cu<sub>3-x</sub>Fe<sub>x</sub>O<sub>7-δ</sub><sup>15</sup> where this transition has been observed for similar values. Irradiation by heavy ions may improve the critical current due to the pinning of the lattice vortices. The epitaxie between substrate and film is, however, modified, as demonstrated by the appearance of the observed reflections (Figure 7, third row) after irradiation with Xe-ions. The evolution of the electron density as a function of dose reveals a gradual degradation of the reflected intensity and even a rearrangement of the film on the substrate for higher doses.

## TRANSMISSION ELECTRON MICROSCOPY OF INTERFACES

As stated above, irradiation of superconducting films by accelerated heavy ions may enhance the critical current. Films of  $\text{Bi}_2\text{Sr}_2\text{CaCu}_2\text{O}_8$  on  $\text{SrTiO}_3$  were irradiated by Au, Xe, and U-ions at the Gesellschaft für Schwerionenforschung, Darmstadt. Doses up to  $10^{12}/\text{cm}^2$  were applied. A channel of amorphous material was thus produced, which acts as an effective pinning centre. Figure 8 shows the relative sharp edge between the

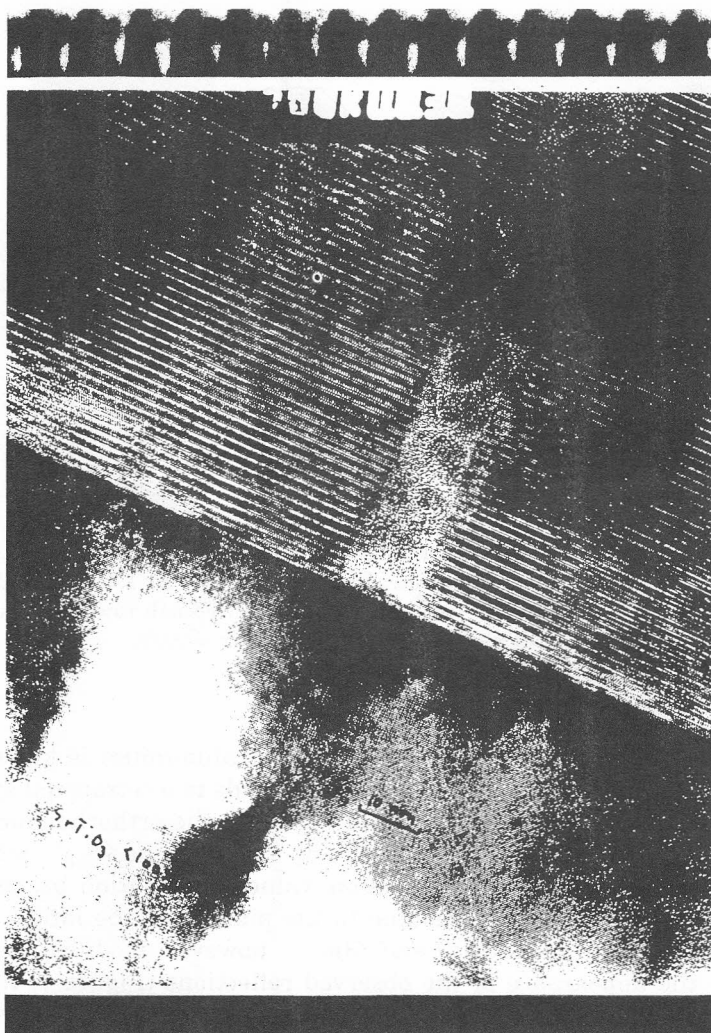


Figure 8. Film of  $\text{Bi}_2\text{Sr}_2\text{CaCu}_2\text{O}_8$  on  $\text{SrTiO}_3$ -substrate, irradiated by U-ions.

channel and the crystal structure of layered material.<sup>16</sup> The radiation damage is considerably less pronounced in the substrate. High resolution electron microscopy was also applied to elucidate the interface structure of the semiconductor  $\text{CoSi}_2$  on Si. Simulations based on a multislice method were carried out as a function of thickness and defocus (Figure 9), which produced a suitable model for the interface structure. Thus, a model of the interface was elaborated, showing the detailed environment of the atoms at the interface and the gradual change of the structure of Si to the structure of  $\text{CoSi}_2$ .<sup>17</sup> The microstructure of nanocrystalline materials is of particular importance, especially as far as a relation between the interior and the surface is concerned. Distinction between bulk and surface is somehow difficult since about 30% of all atoms have to be considered as the surface for particle sizes of 10–30 nm.

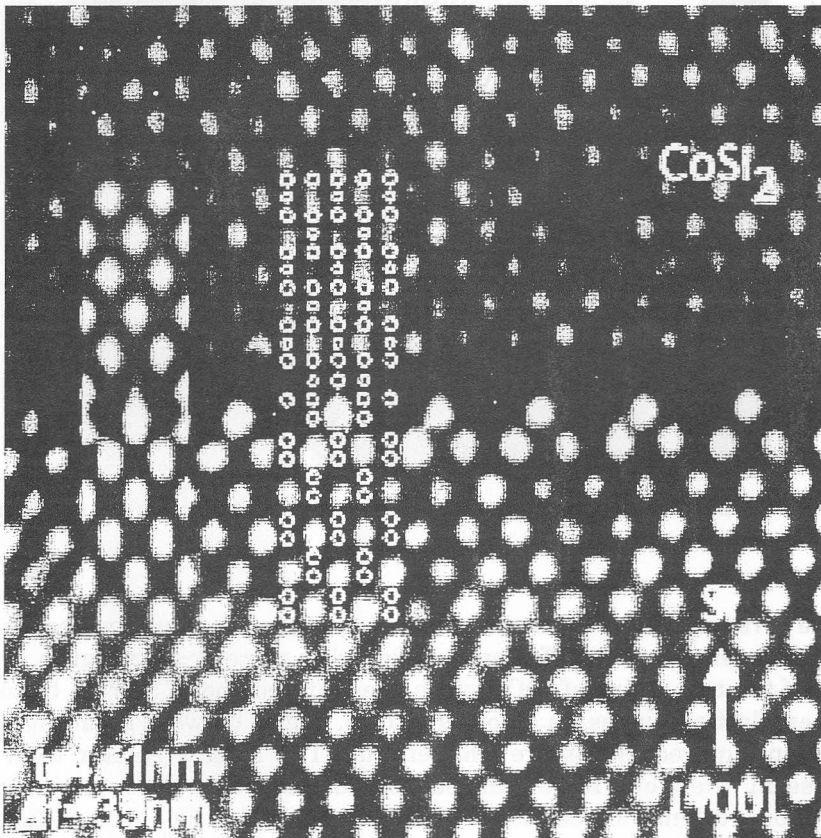


Figure 9. TEM-image of the interface of  $\text{CoSi}_2$  on Si. Inlet: Simulation of interface structure.

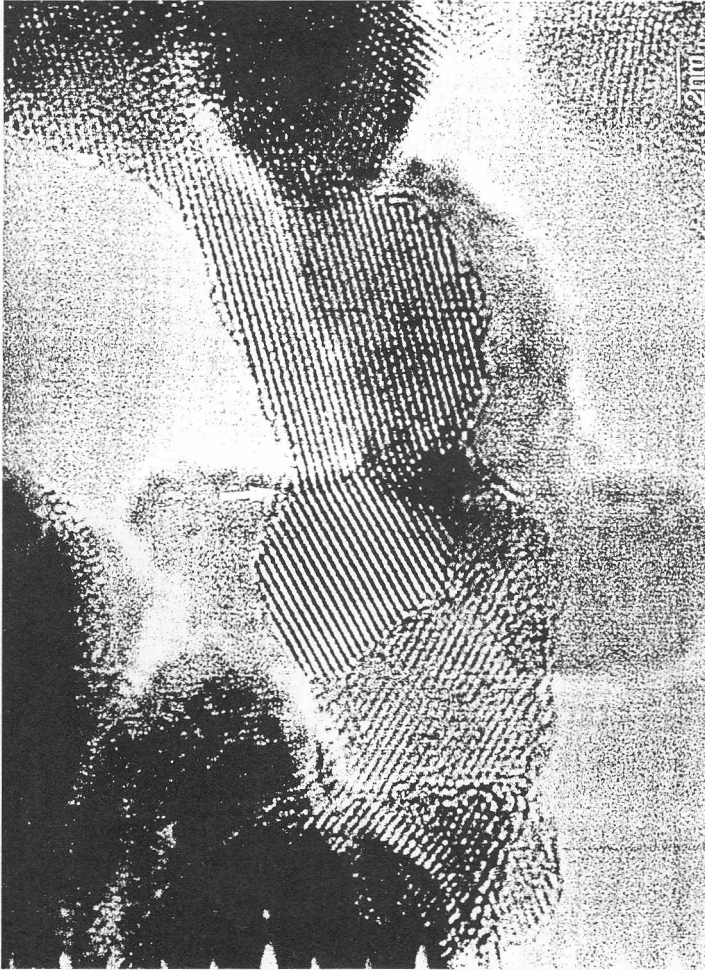


Figure 10. TEM-image of nanocrystalline  $\text{ZrO}_2$  grain boundaries after sintering.

The arrangement of atoms in the surface region is, however, responsible for an understanding of diffusion and sintering processes. In Figure 10, the image of the two grains of  $\text{ZrO}_2$  which are sintered shows a grain boundary with bend lattice fringes. In all observations, angles between adjacent lattice fringes in sintered grains are smaller than  $15^\circ$ . Angles greater than that value seem, therefore, to be unfavourable for sintering. From lattice image simulations, a lense shaped form of the nanoparticles has been deduced. A careful study of lattice image simulations revealed a difference between the structure in the interior of a grain and at the surface, a difference possibly due to different modifications of  $\text{ZrO}_2$ .<sup>18</sup>

MAGNETIC PROPERTIES OF SUPERCONDUCTORS

The copper ions in yttrium barium cuprate (YBCO) occupy two different crystallographic sites, which are named Cu(1) and Cu(2) in the literature. The crystal chemistry of this system has been discussed in many details and will not be repeated here. Substitution of Cu by other 3d-elements (Fe, Co, Ni) or trivalent cations like Al takes place in most cases in the Cu(1)-position. The magnetic ordering of Cu in YBCO was established, and an antiferromagnetic spin arrangement was detected. Furthermore, a phase transition from one antiferromagnetic structure (AF I) to another at low temperature (AF II) was reported. Careful neutron diffraction studies on an Al-doped single crystal of YBCO and on a crystal of undoped material were recently carried out by our group in collaboration with Riso National Labo-

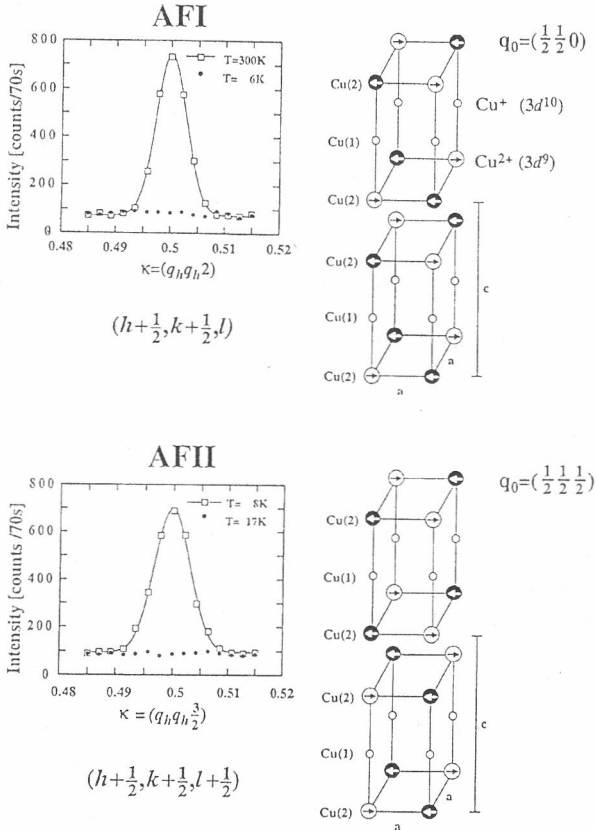


Figure 11. Antiferromagnetic structure of Al-doped YBCO. Above: Intensity of magnetic  $h + 1/2, k + 1/2, l$ -reflection and model of AF I. Below: Intensity of  $h + 1/2, k + 1/2, l + 1/2$  reflection and model of AF II structure.

ratory in Denmark. It was demonstrated that the magnetic phase transition only occurs for the doped material.<sup>19</sup> No such transition was observed for the undoped material<sup>20</sup> in contrast to previous reports. The only possible explanation for that finding is the conclusion that the material previously described was most probably contaminated by Al which occurred in those materials as a consequence of crystal growth in corundum crucibles.

The magnetic structure of the doped material is presented in Figure 11 for the two phases. Only Cu(2)-atoms are involved and carry a magnetic moment of  $\mu \approx 0.5 \mu_B$ . No moment of Cu(1) is observed and an examination of the intensity of the nonmagnetic reflections by neutron and X-ray reflections revealed a replacement of Cu(1) by Al atoms. As Al possibly can not adapt to the linear chain arrangement of Cu(1) but prefers tetrahedral environment, a cluster model for the Al ordering has been proposed which has been checked for various oxidation-reduction conditions.<sup>21</sup>

## CONCLUSION

Crystallographic techniques and methods have a considerable impact on the precise determination of structural details. As the details of the microstructure influence physical and chemical properties of materials to a great extent, crystallographic methods have to be developed further in all fields of materials science.

*Acknowledgement.* – The work presented has been supported by the Deutsche Forschungsgemeinschaft, the Bundesminister für Forschung und Technologie and the Fonds der Chemischen Industrie, Germany.

## REFERENCES

1. H. Fuess, in: *Forschung mit Röntgenstrahlen*, F. H. W. Heuck u. E. Macherauch (Eds.), Springer-Verlag Heidelberg, 1995, pp. 386–401.
2. R. Schnell and H. Fuess, *Ber. Bunsenges. Phys. Chem.* **100** (1996) 578–584.
3. R. Hoppe, G. Schulz-Ekloff, D. Wöhrle, C. Kirschhock, H. Fuess, L. Uytterhoeven, and R. A. Schoonheydt, *Adv. Materials* **7** (1995) 61–64.
4. J. Caro, C. Finger, J. Richter-Mendau, L. Werner, and B. Zibrowius, *Adv. Materials* **4** (1992) 273–276.
5. V. Kaučič, *Croat. Chem. Acta* **67** (1994) 241–287.
6. C. Kirschhock and H. Fuess, *Zeolites*, in press.
7. H. Klein, C. Kirschhock, and H. Fuess, *J. Phys. Chem.* **98** (1994) 12345–12360.
8. C. Kirschhock and H. Fuess, *Microporous Materials* **2** (1994) 261–267.
9. M. Czjzek, H. Jobic, and M. Bee, *J. Chem. Soc., Faraday Trans.* **87** (1991) 3455–3459.
10. T. Pirling, PhD-Thesis, Technical University, Darmstadt, 1995.
11. F. Jähring and H. Fuess, unpublished results.
12. B. Schulte, M. Maul, W. Becker, H. G. Schlosser, S. Elschner, P. Häusler, and H. Adrian, *Appl. Phys. Lett.* **59** (1991) 869–873.

13. C. Tome-Rosa, G. Jakob, M. Maul, A. Walkenhorst, M. Schmidt, P. Wagner, P. Przyslupski, and H. Adrian, *Physica* **C171** (1991) 231–235.
14. T. Steinborn, H. Adrian, E. Brecht, H. Fuess, M. Maul, G. Miehe, K. Petersen, M. Rao, W. Schmahl, M. Schmitt, C. Traeholt, J. Wiesner, G. Wirth, H. Zandbergen, and J. Zegenhagen, *J. Appl. Crystallogr.* **29** (1996) 125–133.
15. Y. Ren, W. Schmahl, E. Brecht, and H. Fuess, *Physica* **C199** (1992) 414–424.
16. J. Wiesner, C. Traeholt, J. Wen, H. Zandbergen, G. Wirth, H. Fuess, *Physica* **C268** (1996) 161–172.
17. M. Rodewald, Unpublished Results.
18. G. Nitsche, M. Rodewald, G. Skandan, H. Fuess, and H. Hahn, *Nanocryst. Materials* **7** (1996) 535–546.
19. E. Brecht, W. Schmahl, H. Fuess, H. Casalta, P. Schleger, B. Lebech, N. H. Andersen, and Th. Wolf, *Phys. Rev.* **B52** (1995) 9601–9610.
20. H. Casalta, P. Schleger, E. Brecht, W. Montfrooig, N. H. Andersen, B. Lebech, W. Schmahl, H. Fuess, R. Liang, W. N. Hardy, and Th. Wolf, *Physica* **C235** (1994) 1623–1624.
21. E. Brecht, W. W. Schmahl, G. Miehe, M. Rodewald, H. Fuess, N. H. Andersen, J. Hanßmann, and Th. Wolf, *Physica* **C265** (1996) 53–66.

## SAŽETAK

### Doprinos kristalografije znanosti o materijalima

*Hartmut Fuess*

Svojstva materijala važnih u raznim područjima znanosti i tehnike izravno ovise o mikrostrukturi. Kristalografija je znanstvena grana u okviru koje se istražuje mikrostruktura tvari i materijala raznolikim difrakcijskim i spektroskopskim metodama.

U radu se navodi nekoliko primjera iz okvira istraživanja materijala u Tehničkoj visokoj školi u Darmstadtu. Pomoću rentgenske i neutronske difrakcije te spektroskopije NMR i neelastičnog raspršenja neutrona istražuje se struktura i dinamika aromatskih molekula u katalitičkim aktivnim zeolitima.

Površine i granične plohe poluvodiča i tankih poluvodičkih filmova proučavaju se u difrakcijskim metodama, gdje upadno zračenje zatvara mali kut s površinom. Analizom difrakcijske slike izvode se podaci o debljini i faznom sastavu tankog filma i o reljefu površine.

Pomoću transmisijske elektronske mikroskopije (TEM) dobivaju se dodatni podaci o strukturi graničnih ploha, posebnom primjenom simulirajućih slika uzorka podijeljenog u slojeve. Prikazano je istraživanje tankih filmova  $\text{CoSi}_2$  na Si te  $\text{LaB}_6$  na GaAs, uz njihovu modifikaciju zamjenom iona. Opisuje se i povećanje tvrdoće površinskog sloja čelika primjenom implantacije iona (ugljik, dušik). Difrakcijskim metodama, gdje upadno zračenje zatvara mali kut s površinom uzorka, dobivaju se podaci o stvaranju raznih karbida pri različitim dubinama u uzorku. U supravodičkim filmovima  $\text{Bi}_2\text{Sr}_2\text{CaCu}_2\text{O}_8$  na  $\text{SrTiO}_3$  povećana je gustoća električne struje za red veličine uvođenjem praznina (ozračivanje sa (Xe, Au, U)). Primjenom TEM opaženi su amorfnii stupci u uzorku, s jasnim granicama između tih stupaca i neoznačenog dijela uzorka.